Available online at www.scholarsresearchlibrary.com

Scholars Research Library

Archives of Applied Science Research, 2011, 3 (2):213-227

(http://scholarsresearchlibrary.com/archive.html)

ISSN 0975-508X
CODEN (USA) AASRC9

Application of Newly Synthetic HP- Cr-III-Containing Nano-Mica- Clay For Stepwise Remediation of Industrial Water-Drains From Some Toxic Heavy Metals Part-II-Size Cavity Calculations & Silicate Structure Visualization

Khaled M.Elsabawy [a,b,*], Waheed F. El-Hawary [a,c] and A.El.Maghraby [a,d]

[a]*Materials Science& Analytical Units ,Chemistry Department, Faculty of Science, Taif University, Alhawya, Taif - Kingdom of Saudi Arabia*
[b]*Materials Science Unit-Chemistry Department-Faculty of Science, Tanta University-EGYPT*
[c]*Analytical Lab-Chemistry Department-Faculty of Science-Cairo University-EGYPT*
[d]*Refractory & Ceramics Department, National Research Center, El Behooth Str., Dokki, Cairo, EGYPT*

ABSTRACT

Mixed solid state / solution routes were applied to synthesize new family of free-fluoride synthetic clay for water remediation applications. To facilitate the incorporation of the cations the solution route was applied with some hydrothermal conditions and complexing with organic moiety (Ethylene glycol). The sample of synthetic free fluoride –Na-4-mica was having the general formula ($Na_4Mg_6M_4Si_4O_{22}.nH_2O$) where M = Cr^{3+}. Structural and micro-structural properties were monitoring by using both of XRD and SEM evaluating , grain size of the mica bulk was found to be in between 2.27- 3.33 μm which are lower than those reported in literatures. Synthetic clay was tested and applied three time (stepwise) as a cations selective remediator. Analytical investigations were made by using ICP-Ms spectroscopy .Investigations proved that synthetic Cr(III)-type clay has medium-to-strong efficiency as cation selective clay towards heavy metals tested . To confirm the synthesized 4Na-mica with general formula $Na_4Mg_6M_4Si_3AlO_{22}.nH_2O$ that prepared via solution route where M = Cr^{+++} theoretical treatment was made by visualizing of tetrahedrally NaMg –silicates unit cell that considered the main constituent of molecular sieving layers that responsible together with cation exchanging strength (4Na-mica) for removal of investigated heavy metals cations namely($^{201}Hg^{++}$, $^{207}Pb^{++}$, $^{112}Cd^{++}$ and $^{139}La^{+++}$) .

Keywords: Synthesis; Mica clay; Free fluoride; XRD; SEM; ICP-Ms.

INTRODUCTION

Due to the interesting exchange behaviour observed in the high charge micas valuable for practical applications, big efforts have been made in understanding their cation exchange

properties. Specifically, several studies have been performed to characterize the interlayer exchange of a set of hydrated monovalent and divalent metal ions on an ultrafine Na-4-Mica. It was established that the ion exchange is strongly influenced by the size of the complex formed in the aqueous solution, being less effective as the hydrated ionic radius increases [1-3].

Waste streams encountered in mining operations, and various chemical processing industries, contain heavy metals which are non-biodegradable, toxic priority pollutants. Due to their tendency to accumulate in living organisms, causing various diseases and disorders, the treatment methods for metal-bearing effluents are essential for environmental and human health protection. Among numerous commonly used techniques for water purification, adsorption technologies have gained the most attention because of their low cost and easy operation [4-18] .

In recent years, an intensive research was conducted focusing on the selection and/or production of low-cost adsorbents with good metal-binding capacities, which could be utilized as an alternative to the most widely used adsorbent in wastewater treatment-activated carbon. Natural materials of both organic and inorganic nature (such as chitosan, zeolites, minerals, etc) and certain waste products from industrial operations (such as fly ash, coal and oxides) are classified as low-cost adsorbents because they are economical and locally available [19-28] Na-4-mica has much the same composition as natural mica, containing aluminum, silicon, and magnesium. But natural mica also contains potassium ions, which sit in hexagonal holes in the mineral's layers, superimposed upon one another, bonding the sheets tightly together. This "closed" structure makes natural mica a poor ion exchange medium, [1,2].

The high adsorption capacity of such clays described above, together with an exclusive selectivity for harmful divalent and heavy metal captions have converted these samples in a promising material for practical applications [29], [30] and [31]. In particular, the availability of these clays for water decontamination and radioactive waste capture by ion exchange are under intense investigation [32], [33] and [34]. Several synthesis methods have been reported in order to obtain pure Na-4-Mica phase since it was identified by the first time in 1972 by Gregorkiewitz as secondary product from the reaction of augite powder in NaF and MgF_2 melts at 900 °C [35]. Paulus et al. have described an elaborated multi-step process to obtain pure phase mica of much smaller crystal size [36]. Later, Franklin and Lee presented a solid state synthesis procedure in which the crystal size of mica is controlled by selecting the crystallization temperature and reaction time [37].

The major goal of the present article is to investigate efficiency of synthetic free-fluoride meso-porous mica-clay namely ,Cr- -mica clay as cation selective with molecular sieving power towards;

1- Selectivity of some di-valent toxic heavy metals (Hg^{++} ,Pb^{++} and Cd^{++}) .
2- Tri-valent cation exchange of lanthanum species in the high charge Na-*n*-Mica (*n* = 4) is reported for the first time without any pre-swelling step and avoiding the use of long organic ions.
3-Visualizing of tetrahedral Silicates layers and evaluating of cavity size which is responsible for molecular sieving phenomenon in this artificial free-fluoride clay .

MATERIALS AND METHODS

II. A. Clay's synthesis:

The selected samples of synthetic free fluoride –Na-4-mica which having the general formula ($Na_4Mg_6M_4Si_{4-x}Al_xO22.nH_2O$) where M = Cr^{3+} , x = 1 was synthesized by applying solution route and sintering procedure using the molar ratios of $Na_2O.2SiO_2.2H_2O$,Al_2O_3 ,$MgCO_3$ and Cr_2O_3 each of highly pure chemical grade purity The mixture were ground carefully then disolved in few drops of concentrated nitric acid forming nitrate extract which diluted by distill water . The nitrate solution was neutralized by using 45 % urea solution and pH becomes ~ 6 .5.

Mixture I was for sodium silicates solution and mixture II was for rest of component (Al +Mg+ Cr) nitrates according to chemical formula desired . Mixture I was diluted by distill water to be 100 ml then pH was adjusted to be 8.5 concentrated solution of ammonia was added carefully till heavy white precipitate from Metals hydroxide is obtained and the pH must be higher than 8 .The precursor is filtered and washed by 2.5 % ammonium nitrate solution .Mixture II of (Mg+ Cr) was passing through the same treatment but in present of ethylene glycol as complexing agent to produce gelatinous precipitate of metals cations hydroxide precursor .

The Mixture I + Mixture II precursors were forwarded to muffle furnace and calcinations process was performed at 880 °C under a compressed air atmosphere for 15 hrs then reground and pressed into pellets (thickness 0.2 cm and diameter 1.2 cm) under 10 Ton /cm^2. Sintering was carried out under air stream at 1050 °C for 10 hrs.The samples were slowly cooled down (20 °C /hr) till 500 °C and annealed there for 5 hrs under air stream . The furnace is shut off and cooled slowly down to room temperature. Finally the materials are kept in vacuum desiccators over silica gel dryer .

The sample was named as Clay I = $Na_4Mg_6Cr_4Si_3AlO_{22}.nH_2O$. As described in Fig.1 tetrahedral units of silicate are the backbone structure of mica clay indicating that each unit cell surrounded by 4-Na-atoms that can be replaced if it is applied as cations exchanger .

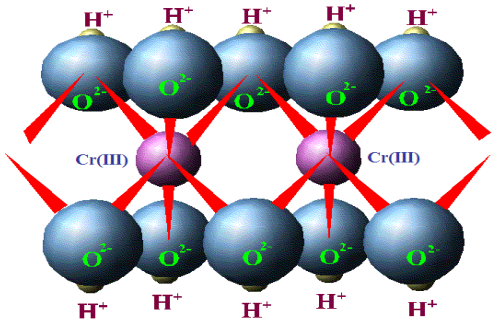

Fig.1 . Structure of Cr-Silicates- Clay

II.B. Phase Identification of Applied Clays :

The X-ray diffraction (XRD) measurements were carried out at room temperature on the fine ground samples using Cu-K_α radiation source,Ni-filter and a computerized STOE diffractometer / Germany with two theta step scan technique .

Scannig Electron Microscopy (SEM) measurements were carried out at different sectors in the prepared samples by using a computerized SEM camera with elemental analyzer unit (PHILIPS-XL 30 ESEM /USA) .

II.C.ICP-MS-Analytical Investigations:

The trace elements ($^{201}Hg^{++}$,$^{207}Pb^{++}$,$^{112}Cd^{++}$ and $^{139}La^{+++}$) were measured with an ICP-MS instrument (ELAN 5000a Perkin Elmer SCIEX ,Norwalk ,CT ,USA) equipped with a standard troch ,cross flow nenbulizer and Ni-sampler skimmer cones .The plasma conditions and measurements parameters applied are listed in the following table.

Table .1: ICP-MS instrument (ELAN 5000a Perkin Elmer operating conditions_

I.ICP-MS Plasma Condition	
Frequency/MHz	40
Rf Forward power/Kw	1.0
Argon gas flow rates ml min^{-1}	
Outer	15
Intermediate	0.8
Nebulizer	0.93-0.98

II.Measurements Parameters :_

-	Resolution	m/z at 10 % peak hight	0.8(normal)
-	Scanning Mode		peak hopping
-	Replicate Time /ms		250
-	Sweeps per Reading		1
-	Reading per Replicate		1
-	Number of Replicates		10
-	Point per Spectral Peak		1

II.C.I. Cation Selectivity &Molecular Sieving Experiment :

The cation exchange and selectivity experiment with clay I (CrIII-clay) was performed by using different three columns each with diameter 1.2 cm^2 and the weight of applied clay was 200 mg in each column .The particle size of applied clay was selected to be $\leq$ 100 µm since the synthesized clay sieved by specific meshes then the column packed with clay .The outlet solution of first step was used as inlet for second remediation step and so on in the third remediation .We believed that the power responsible for remediation and removal of trace elements not only cation exchanging of 4Na-mica but also molecular sieving phenomenon within silicate structure of mica . All standard solutions were standardized to be 10 ppm for each standard by using metal oxide (each of purity $\geq$ 99.9).The standard additions methods with Y-internal references was applied for all investigation .

The experiment was performed at R.T. 27 °C and the rate of flow was adjusted to be five drops /second by using 25 ml separating funnel and the investigated solution was left with clay in the column with continuous shaking for 5 hrs (experiment duration) .

II.C.II. Surface Area Determination of Cr(III)-Clay :

Nitrogen adsorption–desorption isotherms were applied for estimation surface area of synthesized clay . The adsorption isotherms of N_2 were carried out in a Micromeritics ASAP 2000 instrument at −196 °C with a micro-pore system. Specific surface areas were calculated by applying the BET equation to the isotherm. The total volume was considered to be the volume of liquid N_2 adsorbed at a relative pressure of 0.98. The low BET surface area value calculated for this sample – 5 m^2/g– agrees with the situation in which the sodium cations and the interlayer water are fully filling the bidimensional galleries of the aluminosilicate in a non-porous structure. But after the treatment with water, the product gave also a type II isotherm, with a type H4 hysteresis loop, indicative of new slit-shaped meso-porous structure. The increment in the specific BET surface area, up to six times (21.4 m^2/g), is associated with an increment of the external surface between clay domains by the hydrothermal treatment of metal-hydroxide precursors .

RESULTS AND DISCUSSION

III. I. Phase Identification:

Fig. (1_a): displays the X-ray powder diffraction pattern recorded for synthetic free fluoride –Na-4-mica samples which has the general formula ($Na_4Mg_6M_4Si_3AlO_{22}.nH_2O$) where M = Cr^{3+} . The analysis of the corresponding 2θ values and the interplanar spacings d (A°) were carried out using computerized program and indicated that ,the X-ray crystalline structure mainly belongs to a monoclinic phase $Na_4Mg_6M_4Si_3AlO_{22}.nH_2O$ in major besides few peaks of M -silicate . The impurities have been identified as magnesium silicate phase called forsterite (Mg_2SiO_4 JCPDS 34-0189), as clear in Fig.1, and as sodium aluminosilicate phase ($Na_6Al_4Si_4O_{17}$ JCPDS 49-0004) indicated as blue circles . These unit cell parameters are in good agreement with those of the reported ones for $Na_4Mg_6M_4Si_4O_{22}.nH_2O$ structure [6] .

From Figs.1_a one can indicate that monoclinic phase of mica-clay $Na_4Mg_6M_4Si_3AlO_{22}.nH_2O$ is the dominating phase by ratio exceeds than 92 % (d_{100} = 1.2 2 nm) confirming that nano-oxides component are successfully reacted and formed monoclinic biotite phase with very good degree of crystallinity .

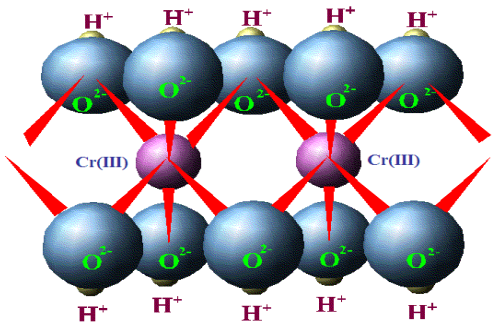

Fig.1 . Structure of Cr-Silicates- Clay

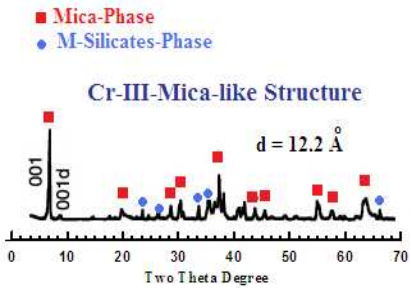

Fig.1$_a$: X-ray diffraction pattern recorded for free-fluoride mica with chemical formula $Na_4Mg_6Cr_4Si_3AlO_{22}.nH_2O$.

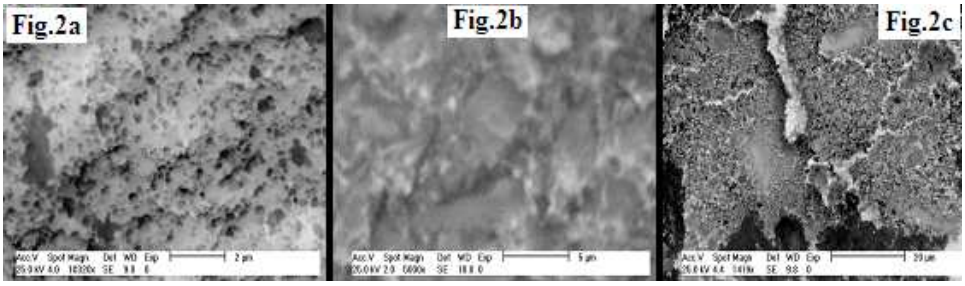

Fig.2$_{a-c}$: SE-micrographs recorded for free-fluoride mica with chemical formula $Na_4Mg_6Cr_4Si_3AlO_{22}.nH_2O$ with different three magnification factors.

The strongest peak observed in the patterns, centred at ≈7.4° 2θ, is attributed to the symmetrical basal [0 0 1] reflection for the hydrated Na-*n*-(Mica) (*n* = 4) with a spacing value of 1.2 nm as clear in Fig.1. Another basal peak of low intensity is also observed in the pattern at a distance of *d* = 0.9 nm – indicated as 001d in the Fig. 1 – which is attributed in the literature to the anhydrous mica phase. The position of the basal peaks is related to the distance between the layers and mainly depends on the layer attraction, nature of the cations present in the interlayer space, the hydration rate of those cations and also on the octahedral character of the M-silicates [38] and [39].

Table.1 explain EDX-elemental analysis data recorded for $Na_4Mg_6M_4Si_3AlO_{22}.nH_2O$ that prepared via solution route .It is clear that the atomic percentage recorded is approximately typical with the molar ratios of prepared sample emphasizing the quality of preparation through solution technique .

On the basis of molar ratio the allowed error in experimental procedures through out solution rout is lesser than those reported in literatures for those synthesized by solid state routes [1,28].

III.II.SE-microscopy measurements :

Fig.(2$_{a-c}$) show the SEM-micrographs recorded $Na_4Mg_6M_4Si_3AlO_{22}.nH_2O$ that prepared via solution route where M = Cr+++ with three different magnification factors . The estimated average of grain size was calculated and found in between 2.27- 3.33 µm supporting the data reported in [23].

The EDX examinations for random spots in the same sample confirmed and are consistent with our XRD analysis for polycrystalline $Na_4Mg_6M_4Si_3AlO_{22}.nH_2O$ that prepared via solution route ,such that the differences in the molar ratios EDX estimated for the same sample is emphasized and an evidence for the existence of monoclinic - phase with good fitting to molar ratios see (Table 1).

From Fig.(2_{a-c}), it is so difficult to observe inhomogeneitiy within the micrograph due to that the powders used are very fine and the particle size estimated is too small.

This indicate that, the actual grain size in the material bulk is smaller than that detected on the surface morphology of the investigated clay.This trend of mismeasuring grain size was observed with [40-41] . Furthermore , particle size was estimated from both of XRD and SEM analyses and its average found to be in between 22-130 nm confiming that solution route synthesis increases the fraction ratio of nano-particles formation .

The surface morphology as clear in Fig.2_a has huge numbers of porous due to the bubling effect resulted from biproduct gases (NH_3 & CO_2) that released during thermal treatment cycle by additional to solution route synthesis with M-hydroxide precursors formed after complexation enhance meso-porous structure which yield to increasing of surface area remarkably .

III.III. Stepwise Remediation Process :

The cation exchange and selectivity experiment with clay I (CrIII-clay) was performed by using different three columns each with diameter 1.2 cm^2 and the weight of applied clay was 200 mg in each column .The particle size of applied clay was selected to be $\leq$ 100 µm since the synthesized clay sieved by specific meshes then the column packed with clay .The outlet solution of first step was used as inlet for second remediation step and so on in the third remediation .

We believed that the power responsible for remediation and removal of trace elements not only cation exchanging of acidic 4Na-mica but also to the molecular sieving phenomenon within silicate structure and in between layers of mica .

Fig.3a shows the cation selectivity of chromium clay towards divalent mercuric ion .It is clear that ~58 % of the standard solution (10 ppm) was captured through the cation exchange process together with molecular sieving in between silicate layers after first remediation cycle ,81 % after 2^{nd} remediation cycle and finally 98.7 % after the third remediation cycle which confirm and reflect superior efficiency of Cr-III-clay towards Hg^{++} ion .
Figs.$3_{b,c}$ show the cation selectivity of chromium clay towards divalent cations of (Pb^{++} ,Cd^{++}), it was noticeable that after 1^{st} remediation process the selectivity ratio was 69 and 75 % , 88 ,89.5 % after 2^{nd} remediation cycle and finally 98.9 ,98.5 % after 3^{rd} remediation cycle respectively .

Although there are no much investigations were found in literatures concerning application of micas clay towards tri-valent cations but in the present investigations we reported cation selectivity and high efficiency of Cr-III-clay towards tri-valent La^{+++} ion as clear in Fig.3_d the selectivity ratios were found 71 ,91.3 and 99.4 % after 1^{st} ,2^{nd} and 3^{rd} remediation cycles respectively .

Figs.4_{a-c} show the remain concentrations in ppm of investigated trace heavy metals namely (Hg^{++} ,Pb^{++} ,Cd^{++} and tri-valent La^{+++}) . It is clear that the remain concentrations after 1st cycle of remediation were 4.2 ,3.1 ,2.5and 2.9 ppm while 1.9 ,1.2 ,1.05 and 0.87 ppm after 2nd remediation cycle and finally 0.13 ,0.11 ,0.14 and 0.06 ppm after 3rd remediation cycle respectively .

From Fig.4_{a-c} and Table .2 one can observe that the net result of La^{+++} remediation is maximum efficiency recording 99.4 % after 3rd cycle of remediation which is a surprise regarding to literatures .

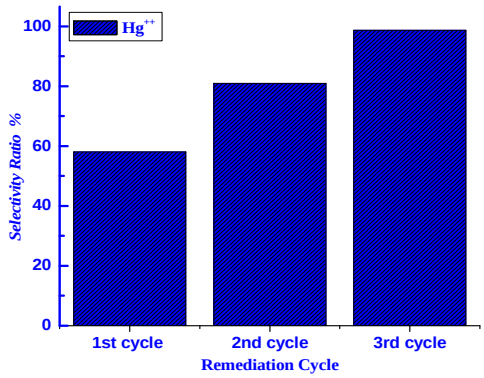

Fig.3_a

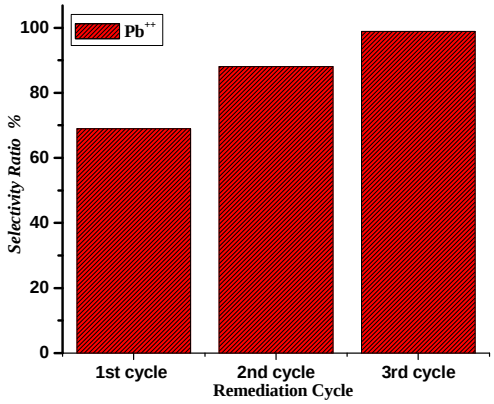

Fig.3_b

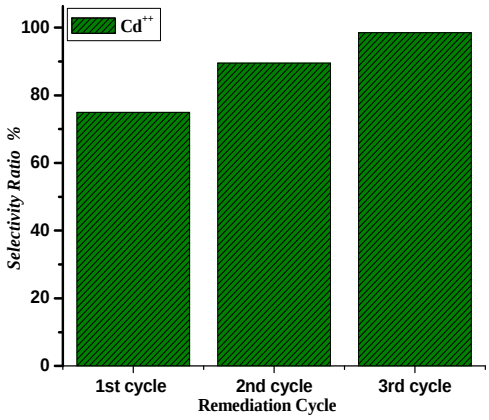

Fig.3_c

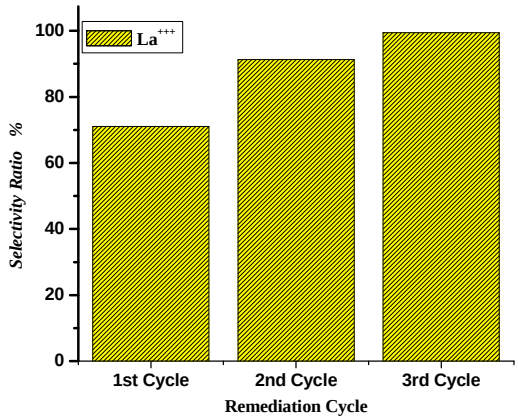

Fig.3_d

Figs.3a-d : Cation selectivity ratio after 1st ,2nd and 3rd remediation cycles for;
a) Hg^{++} (b) Pb^{++}, (c) Cd^{++} and (d) La^{+++} respectively .

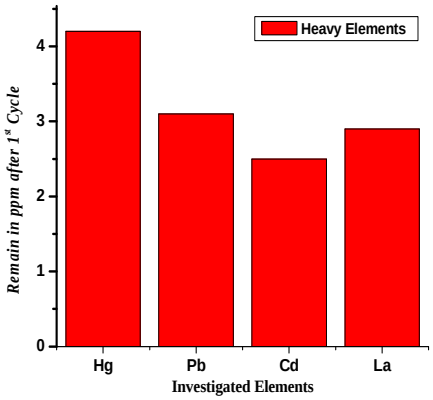

Fig.4$_a$

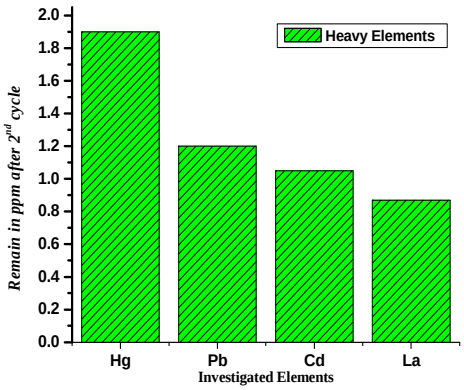

Fig.4$_b$

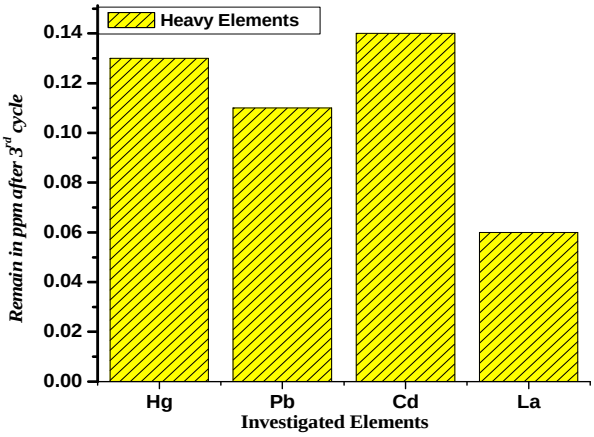

Fig.4$_c$

Figs.4$_{a-c}$: The remain concentration in ppm for tested metals ions after ;
(a) 1st remediation cycle (b) 2nd remediation cycle and (c) 3rd remediation cycle respectively .

This behavior has been related to the difficulty of the cations to diffuse into the narrow interlayer space or to the fact that edges could collapse at the beginning of the process preventing the exchange to proceed. Despite of the detailed study carried out in mono and divalent cations, not much information is available concerning the adsorption behavior of voluminous trivalent cations. In this direction, Shimizu et al. [42] reported the formation of metal oxide pillared clays by intercalation of Fe^{3+} polyhydroxy cations in high charge Na-3-Mica and Na-4-Mica. However, for the ion exchange to be effective a long and tedious pre-swelling step with organoammonium ions was needed to open the layers and facilitate the incorporation of the pillar precursor.

Matching with Shimizu et al. [42] in present investigations ethylene glycol was applied as complexing agent to produce gelatinous meso-porous precipitate of metals cations hydroxide precursor enhancing the layers and facilitate the incorporation of cations even those with tri-valent like La^{+++} . Consequently, an enhancement of stability is expected in those high charge micas from the extra thickness of the non-exchange mica layer in the stratified clay. Despite of

the evident interest for this new family of Cr-III-clays, not much investigation has been pursued in this direction due to two fundamental points: (1) those swelling micas have not shown any affinity for trivalent cations or their hydrolysis products in solution, and (2) the inherent difficulty for the voluminous species to penetrate into the interlayer space.

For the lanthanum to be exchanged, the poly-hydrated cations have to compensate the highly attractive electrostatic forces between the layers to diffuse into the interlayer space. Once the thermodynamic requirement has been satisfied, a quick exchange is expected to occur since diffusion is faster in an already expanded structure.

In the present investigation , the cation exchange of lanthanum species in the high charge Na-*n*-Mica (*n* = 4) is reported for the first time without any pre-swelling step and avoiding the use of long organic ions. To facilitate the incorporation of the cations the solution route was applied with some hydrothermal conditions and complexing with organic moiety (Ethylene glycol) .The diffusion of the hydrated lanthanum through the clay galleries has been confirmed by ICP-Ms investigations see Table .2.

III,IV. Visualizing of Silicate Structure and Estimation of Cavity Size :

To confirm the synthesized 4Na-mica with general formula $Na_4Mg_6M_4Si_3AlO_{22}.nH_2O$ that prepared via solution route where M = Cr^{+++} theoretical treatment was made by visualizing of tetrahedrally NaMg –silicates unit cell that considered the main constituent of molecular sieving layers that responsible together with cation exchanging strength (4Na-mica) for investigated heavy metals cations removal. The visualizing of tetrahedrally NaMg –silicates unit cell (Fig.5) was performed via Diamond Impact Crystal package . The study made was concerned by matching and comparison of calculated and theoretical data as bond distances , oxidation states and bond torsion on the crystal structure formed . The study and comparison between experimental and theoretical data exhibited good fitting of peak positions between experimental and theoretical data confirming that solution route synthesis with some hydrothermal condition lead to mica clay with specific sieving power with certain size cavity .

The analysis of bond distances recorded in Table .3 one can notify that there are no violation on the O1-Si-O1 bond distances observed (~1.725 Å) which reflect that there is no any kind of distortion inside poly–tetrahedrons and consequently lattice structure of silicates .

Furthermore there are no torsions loaded on the bonds angle inside bi-lattice of Na-Mg-Silicates specially O1-Si-O1 angles (136.79°) which reflect stability of non-swelled silicates -mica structure .

The present results are in full agreement with swelling synthetic micas Na-*n*-Mica (*n* = 2, 3 and 4), where *n* is the layer charge per unit cell, which has been successfully synthesized with an unusual cation exchange capacity – up to 468 mequiv./100 g of clay in Na-4-Mica – with up to four monovalent /or two di-valent hydrated cations accommodated in the ditrigonal holes in the external surface of the tetrahedral layer [43]. Despite the large negative charge originated by isomorphic substitution of silicon by chromium in the tetrahedral layer, high charge micas unlike brittle micas, exhibit unexpected structure stability.

We believe that the superior features of removal (Hg^{++} ,Pb^{++},Cd^{++} and La^{+++}) ions from aqueous solution or polluted drains-water after three different remediation cycles is not only due to 4Na-acidic centers that can be replaced as cation axchanger process but also attributable to the molecular sieving and inter-silicates layer calation since the ionic radius of hexa- coordinated radii of investigated cations are (1.02 ,1.19 ,0.95 and 1.03 Å) for (Hg^{++} ,Pb^{++},Cd^{++} and La^{+++}) ions respectively .

As clear in Fig.$_6$ the cavity can be considered as regular hexagon with regular length equal to the base of tetrahedron which is O1-O1 bond length that equal 1.217 Å as clear in Table .3. Accordingly the area of hexagon could be represented as cavity size that mathematically equal to 3.86 $Å^2$.

According to the proposed cavity size which equal to 3.86 $Å^2$ one can understand that hexa-coordinated radii of investigated cations which are (1.02 ,1.19 ,0.95 and 1.03 Å) for (Hg^{++} ,Pb^{++},Cd^{++} and La^{+++}) ions respectively can not penetrate through this cavity size (3.86 $Å^2$) specially if these cations are highly hydrated since the steric-hinderance effect will be high and consequently the molecular sieving efficiency will be increased .

Similar behavior was observed by Shimizu et al. [42]who reported the possibility of formation of metal oxide pillared clays by intercalation of Fe^{3+} poly-hydroxy cations in high charge Na-3-Mica and Na-4-Mica. However, for the ion exchange and sieving strength are effective a long and tedious pre-swelling step with organo-ammonium ions was needed to open the layers and facilitate the incorporation of the pillar precursor and in our case ethylene glycol plays this role .

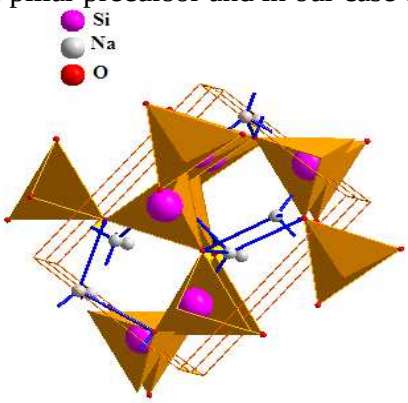

Fig.$_5$: Visualized tetragonal bi-unit cell of Na-Silicates which is the main constituent of Cr-III-Silicate clay.

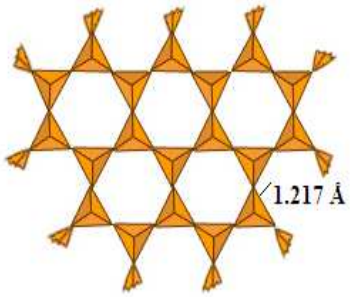

Fig.$_6$. Molecular Sieving Structure of Cr-III-Silicates- Clay

Table.(1) : EDX-Elemental analysis data recorded for Cr-clay-I .

Cr-Clay-I						
Element	Wt %	At %	K-Ratio	Z	A	F
O K	37.81	57.25	0.1069	1.7334	0.1481	1.0804
NaK	18.21	35.13	0.0479	1.1733	0.7353	1.0131
MgK	12.22	16.48	0.2731	1.0746	0.9607	1.0813
Cr L	16.66	16.65	0.0513	0.5181	1.0718	1.1498
Si L	16.98	16.23	0.2364	0.2175	1.0501	1.1212
Al L	3.87	5.331	0.1235	0.1297	0.8650	1.0456

Table. (2):ICP-MS analytical data recorded for three remediation processes .

Cr-ClayI		R(S) ppm	ppm	ppm	ppm R(S)
Clay Type	Composition	Hg^{++}±0.03	Pb^{++}±0.03	Cd^{++}±0.03	La^{+++} ±0.03
1st	$Na_4Mg_6Cr_4Si_3AlO_{22}.nH_2O$	4.2(5.8)	3.1(6.90)	2.5(7.5)	2.9(7.1)
2nd		1.90(2.3)	1.2(1.90)	1.05(1.45)	0.87(2.03)
3rd		0.13(1.77)	0.11(1.09)	0.14(0.91)	0.06(0.81)

R = Remain , (S) = Selective by Clay

Table.3: Selected some bond distances estimated from visualized structure of tetrahedral silicate unit cell .

$Atom_1$-$Atom_2$ A°		Bond length
Si1|Mg1	O1	1.7286
	O1	1.7286
	O1	1.7685
	O1	1.7685
Na1	O1	2.3294
	O1	2.3294
	O1	2.4561
	O1	2.4561
O1	Si1|Mg1	1.7286
	Si1|Mg1	1.7685
	O1	1.2127
	Na1	2.3294
	Na1	2.4561

Table.4: Some selected angles of atom1-^2-3 estimated from visualized structure of tetragonal silicate unit cell .

Atom1^23	Angle °
Si1|Mg -O1-O1	114.534
O1- O1	108.548
O1- O1	109.659
O1-O1	109.659
O1-O1	108.548
O1-O1	105.509
Na1 -O1-O1	139.484
O1-O1	109.155
O1-O1	103.846
O1-O1	103.846

	O1-O1	109.155
	O1-O1	69.946
O1	-Si1|Mg1-O1	136.791
O1	-Si1|Mg1-O1	136.791
O1	-Si1|Mg1-O1	136.791
O1	-Si1|Mg1-Si1|Mg	146.731
O1	-Si1|Mg1-Si1|Mg	146.731
	Si1|Mg1-Na1	121.063
	Si1|Mg1-Na1	103.252
	Si1|Mg1-Na1	100.117
	Si1|Mg1-Na1	92.273
	Na1-Na1	84.672

CONCLUSION

The conclusive remarks inside this article can be briefed as follow ;

1- Solution route with some hydrothermal conditions and complexing with organic moiety (Ethylene glycol) was applied to synthesize -free fluoride- $Na_4Mg_6Cr_4Si_3AlO_{22}.nH_2O$.
2-Cr-III-clay exhibits moderate-to-strong strength as cation selective with molecular sieving power towards ;

a- Selectivity of some di-valent toxic heavy metals (Hg^{++} ,Pb^{++} and Cd^{++}) .
b- Tri-valent cation exchange of lanthanum species in the high charge Na-*n*-Mica (*n* = 4) .

3- Solution route with some hydrothermal conditions yield to specific surface area 21.4 m^2/g which is higher six time than those reported in literatures .

4-SE-micographs with EDX analysis confirmed that free fluoride- $Na_4Mg_6Cr_4Si_3AlO_{22}.nH_2O$ has meso-porous structure with grain size in between 2.27- 3.33 μm and average particle size 22-130 nm confiming that solution route synthesis increases the fraction ratio of nano-particles formation .

4- The cavity size was estimated to be equal to 3.86 $Å^2$ and hexa- coordinated radii of investigated cations which are (1.02 ,1.19 ,0.95 and 1.03 Å) for (Hg^{++} ,Pb^{++},Cd^{++} and La^{+++}) ions respectively can not penetrate through this cavity size (3.86 $Å^2$) specially if these cations are highly hydrated since the steric-hinderance effect will be high and consequently the molecular sieving efficiency will be increased .

REFERENCES

[1] R.E. Grim, Clay Mineralogy, McGraw-Hill Book Company, New York **(1968)**,pp. 596.
[2] M. Gregorkiewitz and J.A. Rausell-Colom, *Am. Mineral.* 72 **(1987),** pp. 515.
[3] T. Kodama and S. Komarneni, *J. Mater. Chem.* 9 **(1999)**, pp. 533.
[4] M.A. Al-Ghouti, M.A.M. Khraisheh and M. Tutuji, *Chemical Engineering Journal* 104 (1–3) **(2004),** pp. 83–91.

[5] S.J. Allen and B. Koumanova, *Journal of the University of Chemical Technology and Metallurgy* 40 (3) **(2005),** pp. 175–192.
[6] S. Aytas, S. Akyil, M.A.A. Aslani and U. Aytekin, *Journal of Radioanalytical and Nuclear Chemistry* 240 (3) **(1999),** pp. 973–976.
[7] S. Babel and T.A. Kurniawan, *Journal of Hazardous Materials* B97 (1–3) **(2003)**, pp. 219–243.
[8] E.P. Barrett, L.G. Youner and P. Halenda, *Journal of the American Chemical Society* 73 (1) **(1951),** pp. 373–380.
[9] K.G. Bhattacharyya and S.S. Gupta, *Journal of Colloid and Interface Science* 310 (2) **(2007),** pp. 411–424.
[10] C. Camilo, G. Carmen and M. Paula, *Journal of Chemical Technology & Biotechnology* 80 (4) **(2005),** pp. 477–481.
[11] J.M. Charnock, K.E.R. England, M.L. Farquhar and D.J. Vaughan, , *Physica. B, Condensed Matter* 208–209 **(1995)**, pp. 457–458.
[12] T.N.D. Dantas, A.A.D. Neto and M.C.P. Moura , *Water Research* 35 (9) **(2001)**, pp. 2219–2224.
[13] M.K. Doula and A. Ioannou, *Microporous and Mesoporous Materials* 58 (2) **(2003),** pp. 115–130.
[14] F. Ekmekyapar, A. Aslan, Y.K. Bayhan and A. Cakici, Biosorption of copper(II) by nonliving lichen biomass of *Cladonia rangiformis* Hoffm, *Journal of Hazardous Materials* 137 (1) **(2006),** pp. 293–298.
[15] E. Erdem, N. Karapinar and R. Donat, *Journal of Colloid and Interface Science* 280 (2) **(2004)**, pp. 309–314.
[16] O. Hamdaouia and E. Naffrechoux, *Journal of Hazardous Materials* 147 (1–2) **(2007)**, pp. 381– 394.
[17] Y.S. Ho, J.F. Porter and G. McKay, *Water, Air, and Soil Pollution* 141 (1–4) **(2002),** pp. 1–33.
[18] IPCS (International Programme on Chemical Safety) **1998**. Copper. Environmental Health Criteria 200. Geneva, Switzerland: World Health Organization **(1998).**
[19] A. Kayaa and A.H. Oren, *Journal of Hazardous Materials* B125 (1–3) **(2005),** pp. 183–189.
[20] M.A.M. Khraisheh, Y.S. Al-degs and W.A.M. Mcminn, *Chemical Engineering Journal* 99 (2) (2004), pp. 177–184.
[21] S. Kubilay, R. Gürkan, A. Savran and T. Şahan, *Adsorption* 13 (1) **(2007)**, pp. 41–51.
[22] S. Lazarević, I. Janković-Častvan, D. Jovanović, S. Milonjić, Dj. Janaćković and R. Petrović, *Applied Clay Science* 37 (1–2) **(2007)**, pp. 47–57.
[23] S.-H. Lin and R.-S. Juang, *Journal of Hazardous Materials* B92 (3) **(2002),** pp. 315–326.
[24] N. Meunier, J. Laroulandie, J.F. Blais and R.D. Tyagi, *Bioresource Technology* 90 (3) **(2003),** pp. 255–263.
[26] T. Mishra and S.K. Tiwari, Studies on sorption properties of zeolite derived from Indian fly ash, *Journal of Hazardous Materials B* 137 (1) **(2006),** pp. 299–303.
[27] A.E. Osmanlioglu, *Applied Radiation and Isotopes* 65 (1) **(2007),** pp. 17–20.
[28] M. Panayotova and B. Velikov, Kinetics of heavy metal ions removal by use of natural zeolite, *Journal of Environmental Science and Health A* 37 (2) **(2002),** pp. 139–147.
[29] T. Kodama and S. Komarneni, *J. Mater. Chem.* 9 **(1999),** p. 533.
[30] T. Kodama, S. Komarneni, W. Hoffbauer and H. Schneider, *J. Mater. Chem.* 10 **(2000)**, p. 1649.

[31] T. Kodama, Y. Harada, M. Ueda, K. Shimizu, K. Shuto and S. Komarneni, *Langmuir* 17 **(2001)**, p. 4881
[32] R. Ravella, S. Komarneni and C. Enid-Martínez, *Environ. Sci. Technol.* 42 **(2008)**, p. 113.
[33] M.D. Alba, M.A. Castro, M. Naranjo and E. Pavón, *Chem. Mater.* 18 **(2006)**, p. 2867.
[34] S. Komarneni, N. Kozai and W.J. Paulus, *Nature* 410 **(2001),** pp. 771
[35] M. Gregorkiewitz, Zur Darstellung von Tektosilicaten in Salzschemelzen, Diplomarbeit, Universität München, Germany, **1972.**
[36] W.J. Paulus, S. Komarneni and R. Roy, *Nature* 357 **(1992)**, pp. 571.
[37] K.R. Franklin and E. Lee, *J. Mater. Chem.* 6 **(1996)**, pp. 109.
[38] G.W. Brindley and F.H. Gillery, *Am. Mineral.* 41 **(1956)**, pp. 169.
[39] J. Davitdtz and P.F. Low, *Clay Clay Miner.* 18 **(1970)**, pp. 325.
[40] Khaled M.Elsabawy, *Physica C* 432**(2005)**pp.263-269.
[41] Khaled M. Elsabawy and Elsayed E. Kandyel ,*Materials Research Bulletin,* 42, 6, 5 **(2007)** 1051-1060
[42] K. Shimizu, Y. Nakamuro, R. Yamanaka, T. Hatamachi and T. Kodama, *Micropor. Mesopor. Mater.* 95 **(2006)**, pp. 135.
[43] M. Gregorkiewitz and J.A. Rausell-Colom, *Am. Mineral.* 72 **(1987**), pp. 515.